FULLY AUTOMATED MOSAICKING OF PUSHBROOM AERIAL IMAGERY

Claude Cariou, Kacem Chehdi

TSI2M Laboratory - ENSSAT/University of Rennes 1
6, rue de Kerampont, BP 80518
22305 Lannion, France

ABSTRACT

This communication addresses the problem of the automatic mosaicking of raw images acquired by airborne pushbroom imagers. Using appropriate ancillary data issued from GPS and inertial measurements, we show how the mutual information criterion can be used to improve the co-registration and direct georeferencing of overlapping flight lines by estimating unknown or inaccurate elevation data. The proposed approach does not require any control point to work, and requires only few iterations to improve the initial pose. The mosaicking task itself is performed in a very simple manner. We describe the proposed system, and assess the robustness of our method with an example of application to the mosaicking of multi-track real multispectral image data.

***Index Terms*—** Information theory, Image registration, Variational methods, Image processing, Geometry

1. INTRODUCTION

Mosaicking of Earth Observation (EO) images is the task of combining several images into an image mosaic which covers a large area and therefore can be used for mapping, land use classification, and change detection [1] [2]. Although image mosaicking is frequently performed for spaceborne imagery, the case of airborne multi- / hyper-spectral pushbroom imaging systems is very challenging due to (i) atmospheric turbulence with effects on the external orientation of the camera; (ii) variations of the terrain height; (iii) variations in the spectral radiance for same targets under different viewing conditions [3] [4] [5]. Traditionally, the mosaicking of raw images acquired by pushbroom imagers such as CASI, AISA, or AVIRIS is performed only once the georeferencing step is done for every image to be included in the mosaic. Georeferencing is the way of providing accurate coordinates in a given geodetic or map coordinate system to pixels of remotely sensed images. In the case of aerial pushbroom imagers there are two ways of performing the georeferencing: the first one is based on the use of a set of ground control points and image points from which adequate interpolation procedures are used to georectify the raw distorted image [6]. The second one which is mostly used is called *direct georeferencing* [7]. It requires a set of ancillary data related to the exterior orientation of the pushbroom imager and collected jointly with the raw image. These data are then mixed up in a post-acquisition processing to produce the georectified/georeferenced image. The set of ancillary data is acquired by a GPS/INS (inertial navigation system) and provides the position (typically in Lat/Lon), the height above the reference ellipsoid (typically WGS84) and the attitude parameters (in roll, pitch and yaw) of the aircraft for each scan line of the raw image. However, this dataset is generally not sufficient to provide accurate positioning in the geocorrected image, and it is necessary to use a digital elevation model (DEM) in order to achieve sufficient accuracy (typically sub-pixel to few pixels RMS error), especially for wide angle cameras.

One problem with direct georeferencing relies in the accuracy of the ancillary data and the DEM. Indeed, some of the positioning or aircraft attitude measurements may be altered by systematic errors which should be accounted for. Moreover, the DEM data is not always available or may not be enough accurate.

In this communication, we address the problem of the automatic mosaicking of images acquired by airborne pushbroom imagers. The step of co-registration of contiguous flight strips is emphasized, since it is the most difficult. In order to perform accurate registration of raw images without defining control points, we suggest the use of the mutual information criterion into a variational approach setting, aiming at the estimation of an unknown DEM.

In Section 2, we will describe our approach in detail. In Section 3, we will present some experimental results involving data acquired by an AISA Eagle pushbroom imager. A conclusion will be given in Section 4.

2. PROPOSED MOSAICKING APPROACH

2.1. Deformation model

The automatic registration of a raw image acquired by a multispectral scanner onto a reference image requires a precise modeling of the deformation processes which are involved.

This work is supported by the Regional Council of Brittany and the European Union through the Leader+ Programme.

Let us define $\Omega = \Omega_i \times \Omega_j$ as the set of coordinates of a raw image. $\Omega_i = \{1, \ldots, N\}$ is the set of across-track coordinates, and $\Omega_j = \{1, \ldots, M\}$ is the set of along-track coordinates. From classical photogrammetry [8], it can be shown that the ground coordinates (x_{ij}, y_{ij}) of a pixel with coordinates (i, j) in the raw image are given by:

$$\begin{bmatrix} x_{ij} \\ y_{ij} \end{bmatrix} = \begin{bmatrix} \cos\theta_j & -\sin\theta_j \\ \sin\theta_j & \cos\theta_j \end{bmatrix} \begin{bmatrix} X'_{ij} \\ Y'_{ij} \end{bmatrix} + \begin{bmatrix} X_j \\ Y_j \end{bmatrix} , \quad (1)$$

with θ_j the instantaneous aircraft heading and (X'_{ij}, Y'_{ij}) the relative unreferenced and unoriented ground pixel coordinates

$$\begin{bmatrix} X'_{ij} \\ Y'_{ij} \end{bmatrix} = \begin{bmatrix} (z_{ij} - Z_j)\frac{r_{12,j}c_i - r_{13,j}}{r_{32,j}c_i - r_{33,j}} \\ (z_{ij} - Z_j)\frac{r_{22,j}c_i - r_{23,j}}{r_{32,j}c_i - r_{33,j}} \end{bmatrix} , \quad (2)$$

with $\mathbf{z} = [\{z_{ij}\}]_{i\in\Omega_i, j\in\Omega_j}$ the topographic height of the imaged scene; $[\mathbf{XYZ}] = [\{X_j\}; \{Y_j\}; \{Z_j\}]^T_{j\in\Omega_j}$ are the locations of the sensor in an arbitrary coordinate system (for instance, X is the position in Easting, Y is the position in Northing, and Z is the height above the ground level); $c_i = \tan(\frac{FOV}{2})\frac{2(i-i_0)}{N}$ where i_0 is the index of the pixel located at the principal point in the image plane and FOV is the field of view of the pushbroom sensor; the coefficients r_{kl} are given by the 3-D rotation matrix for each scan line j:

$$\begin{bmatrix} r_{11,j} & r_{12,j} & r_{13,j} \\ r_{21,j} & r_{22,j} & r_{23,j} \\ r_{31,j} & r_{32,j} & r_{33,j} \end{bmatrix} = \begin{bmatrix} 1 & 0 & 0 \\ 0 & \cos\omega_j & -\sin\omega_j \\ 0 & \sin\omega_j & \cos\omega_j \end{bmatrix} .$$
$$\begin{bmatrix} \cos\phi_j & 0 & \sin\phi_j \\ 0 & 1 & 0 \\ -\sin\phi_j & 0 & \cos\phi_j \end{bmatrix} . \begin{bmatrix} \cos\kappa_j & \sin\kappa_j & 0 \\ -\sin\kappa_j & \cos\kappa_j & 0 \\ 0 & 0 & 1 \end{bmatrix} , \quad (3)$$

where ω_j, ϕ_j and κ_j are the instantaneous absolute values of respectively the roll, pitch and yaw angles of the aircraft which define the external orientation of the camera.

Summarizing, the georeferencing of every pixel in a raw (deformed) image is possible as soon as the whole deformation process $\mathcal{D}(\mathbf{X}, \mathbf{Y}, \mathbf{Z}, \omega, \phi, \kappa, \mathbf{z})$ is known. In the following, we will consider that all the ancillary data is available and accurate, but the DEM (or equivalently $\mathbf{z}$) is not available or inaccurate on the area where two or more flight tracks are to be mosaicked. Note that the $\mathbf{z}$ data is in fact an interpolation of the georeferenced DEM w.r.t. the current deformation process.

2.2. Mutual information comparison functional

Aerial surveys over large areas and involving several flight tracks are often performed in a short time slot (typically up to two hours) in order to overcome bidirectional reflectance distribution function (BRDF) effects with varying viewing and sun incidence angles [2]. Indeed, BRDF effects are known to alter the radiance of target materials, making difficult tasks such as land use classification. Therefore, overlapping regions imaged at different times and from different position may not look similar in radiance, which makes image comparison functionals such as the means squared error or the correlation ratio useless. In such a case, the use of the mutual information between images should be preferred [9] [10] [11].

Let $\mathcal{D}_1$ and $\mathcal{D}_2$ the deformation processes which give rise to raw images I_1 and I_2, respectively, and corresponding to adjacent flight tracks. We have considered the maximization of the following criterion w.r.t. the unknown DEM:

$$\mathcal{J}_{\mathcal{MI}}(\text{DEM}) = \mathcal{MI}(I_1, I_2 \circ \mathcal{D}_2^{-1} \circ \mathcal{D}_1) \quad , \quad (4)$$

where the mutual information between two images I_1 and I_2 is given by:

$$\mathcal{MI}(I_1, I_2) = \int_{\mathbb{R}^2} f_{I_1,I_2}(u,v) \log \frac{f_{I_1,I_2}(u,v)}{f_{I_1}(u) f_{I_2}(v)} du dv \quad (5)$$

f_{I_1,I_2} represents the joint pdf of images I_1 and I_2, and f_{I_1} and f_{I_2} are the marginal pdfs.

Note that $I_2 \circ \mathcal{D}_2^{-1} \circ \mathcal{D}_1$ is supposed to align more or less with I_1: I_2 is first geocorrected by the inverse deformation process $\mathcal{D}_2^{-1}$ and then interpolated by the direct deformation process $\mathcal{D}_1$.

2.3. Optimization by variational approach

Optimizing Eq. (4) w.r.t. the unknown DEM is a difficult task due to the high nonlinearity of the image formation processes. This is why we have performed the optimization of the DEM by a variational method, approximating elevation variations by filtered weighted gradients of the current image $I_c(\mathbf{z}_1) = I_2 \circ \mathcal{D}_2^{-1} \circ \mathcal{D}_1(\mathbf{z}_1)$. More precisely, the gradient flow we have set up writes:

$$\begin{cases} (\mathbf{z}_1)_t = \left[-\frac{1}{|\Omega|} \left[\psi * \frac{\partial L^{\mathbf{z}_1}}{\partial v} \right] (I_1, I_c(\mathbf{z}_1)) \, \nabla_i I_c(\mathbf{z}_1) \right] \\ \qquad\qquad * \, \mathbf{g} \\ \mathbf{z}_1|_{t=0} = \mathbf{z}_{1_0} \end{cases} \quad (6)$$

where

$$\frac{\partial L^{\mathbf{z}_1}}{\partial v} = \frac{1}{f_{I_1,I_c(\mathbf{z}_1)}(u,v)} \frac{\partial f_{I_1,I_c(\mathbf{z}_1)}(u,v)}{\partial v} - \frac{1}{f_{I_c(\mathbf{z}_1)}(v)} \frac{\partial f_{I_c(\mathbf{z}_1)}(v)}{\partial v} \quad , \quad (7)$$

ψ is the kernel used to smooth the joint pdf $f_{I_1,I_c(\mathbf{z}_1)}$, and $\mathbf{g}$ represents the impulse response of a 2-D low-pass filter used to regularize the solution. The initial $\mathbf{z}_{1_0}$ can be chosen as either a constant or an interpolation of an approximate DEM when available. Note that the gradient used is relative to the coordinate index i, because the difference between I_1 and I_c which is induced by inaccurate elevation data is prominent in the across-track direction.

2.4. Co-registration system for DEM estimation

Figure 1 depicts the system which was finally implemented for the co-registration of two adjacent flight tracks. The system was divided into processing blocks. The `NAV` block computes ground map coordinates $(\mathbf{x}, \mathbf{y})$ from the ancillary and DEM data using Eqs. (1)-(3) for both images. The `GeoRef` block performs the georeferencing of raw images, i.e. drapes these into the chosen coordinate system. The `Interpol` block interpolates a georeferenced image with a given set of map coordinates and is in fact the reverse of the `GeoRef` function. Finally, the `Mutual Info` block computes the variations in the $\mathbf{z}_1$ data in Eq. (6) from which a variation of the dDEM is added to the initial DEM_0 to provide the current estimate $\widehat{\text{DEM}}$.

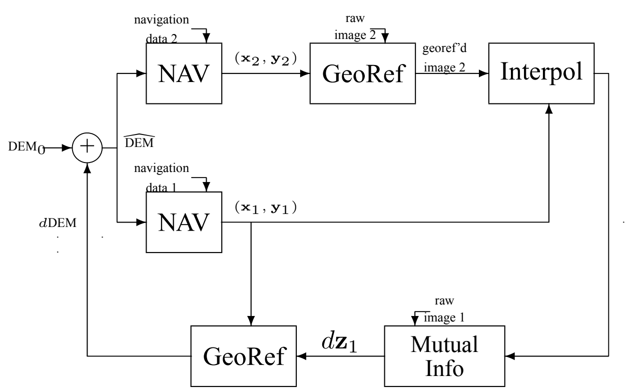

Fig. 1. DEM estimation from overlapping image data with associate ancillary measurements.

2.5. Radiance correction procedure

The mosaicking of overlapping remote sensing images is usually performed by selecting at each pixel location the radiance value(s) from one of the two registered images. This simple scheme, which we have used in our experiments, moreover avoids the mixing of data which can severely alter the expected mosaic. However, due to BRDF effects, the alignment of intensity values at registered pixel sites in a given spectral band is highly unlikely, but generally follows a linear function with a good correlation ratio. Hence, we have developed a procedure which computes the mean proportionality coefficient between individual pixel radiances belonging to adjacent images. This multiplicative coefficient was then applied to normalize intensity values of one image w.r.t. the other one.

3. EXPERIMENTAL RESULTS

In order to assess the proposed scheme, we have first performed the mosaicking of two flight tracks acquired May 11, 2007 in the region of Le Mans, France, using the hyperspectral system AISA Eagle in full swath mode. The objective of this survey was multiple, including the detection of diseases in barley crops and the harvest forecast of peas and wheat. Raw images I_1 and I_2 are both 955 $\times$ 2200 pixels. Figure 2 shows an overlay of two adjacent image strips I_1 and I_c in their initial pose, i.e. without DEM refinement. In this case the initial DEM was set up constant with 120 meters height above the mean sea level. The co-registration system described above was run for 15 iterations. The final estimate of $\mathbf{z}_1$ in Figure 2-(c) shows height values in the range $[123-140]$ meters. Note that the upper part of the final $\mathbf{z}_1$ remains at the initial altitude, i.e. 120 meters. To assess the co-registration, we have computed the RMS location error using 20 control points between I_1 and the initial $I_c(\mathbf{z}_{1_0})$ first, and then the final $I_c(\mathbf{z}_1)$. The RMS error has shown to decrease from 11.50 pixels to 3.13 pixels after processing, which proves the efficiency of our approach.

Finally we have performed a full mosaicking of a set of six flight tracks acquired over a coastal zone located in Lanros, Brittany, France, with true elevation data in the range $[0 - 30]$ meters. The DEM data was constructed by adding contributions of DEM corrections from one track to another in a forward-backward scheme. Our system was started using a zero DEM. Figure 3 shows the final DEM estimate as well as the corresponding SRTM DEM available from the Seamless Data Distribution System for comparison [12]. Despite its smoothness, our DEM estimate was able to detect a mound in the upper right part of the mosaic, which is not present in the SRTM data. Original (without DEM) and final mosaics are also given and show the improvement in co-registration and radiance alignment brought by our approach. The planimetric RMS error computed from 100 control points on overlapping images is around 3 pixels and the altimetric RMS error between our DEM estimate and the SRTM DEM is below 10 meters.

4. CONCLUSION

In this communication, we have described a system which allows the automatic mosaicking of pushbroom optical remote sensing images. This system accounts for the large deformation processes which occur in aerial imaging and automatically corrects the direct georeferencing step for unknown elevation variations by a mutual information approach, which avoids the use of any control points between adjacent flight tracks. The optimization of the criterion is performed by a variational method. The radiance correction step itself is performed in a simple fashion based on a linear regression of radiance measurements between adjacent images. Extensions

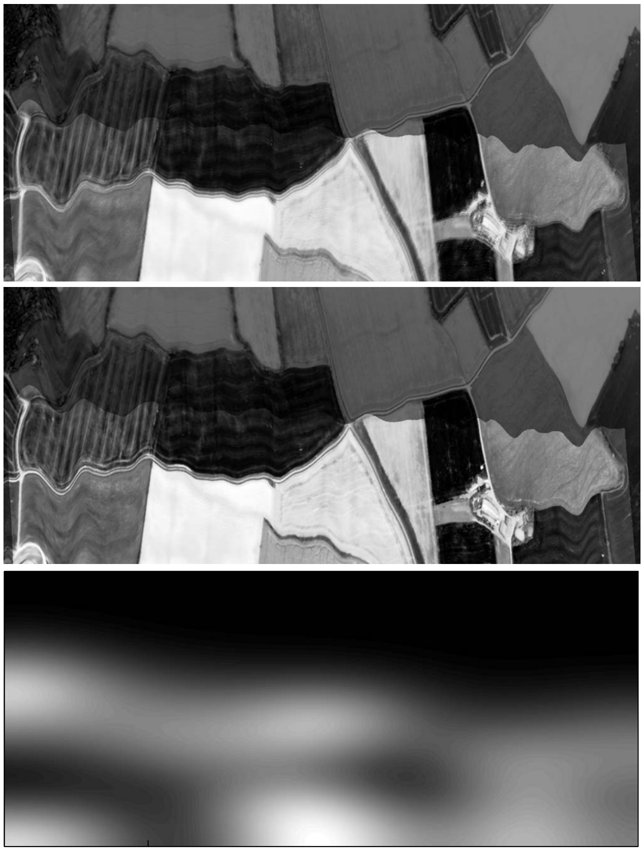

Fig. 2. Automatic registration of adjacent flight tracks: Top: initial pose ; middle: final pose ; bottom: final estimate of $\mathbf{z}_1$ obtained from the gradient flow in Eq. (6).

of this work are foreseen concerning the estimation of unknown or inaccurate flight parameters such as boresight angles and drifts.

5. REFERENCES

[1] S. Leprince *et al.*, "Automatic and precise orthorectification, coregistration, and subpixel correlation of satellite images, application to ground deformation measurements," *IEEE Transactions on Geoscience and Remote Sensing*, vol. 45, no. 6, pp. 1529–1558, June 2007.

[2] S. Tuominen and A. Pekkarinen, "Local radiometric correction of digital aerial photographs for multi source forest inventory," *Remote Sensing of Environment*, vol. 89, no. 1, pp. 72–82, January 2004.

[3] D. Schlaepfer and R. Richter, "Geo-atmospheric processing of airborne imaging spectrometry data part 1: Parametric orthorectification.," *International Journal of Remote Sensing*, vol. 23, no. 13, pp. 2609–2630, 2002.

[4] R. Richter and D. Schlaepfer, "Geo-atmospheric processing of airborne imaging spectrometry data part 1: Part 2: Atmospheric/topographic correction.," *International Journal of Remote Sensing*, vol. 23, no. 13, pp. 2631–2649, 2002.

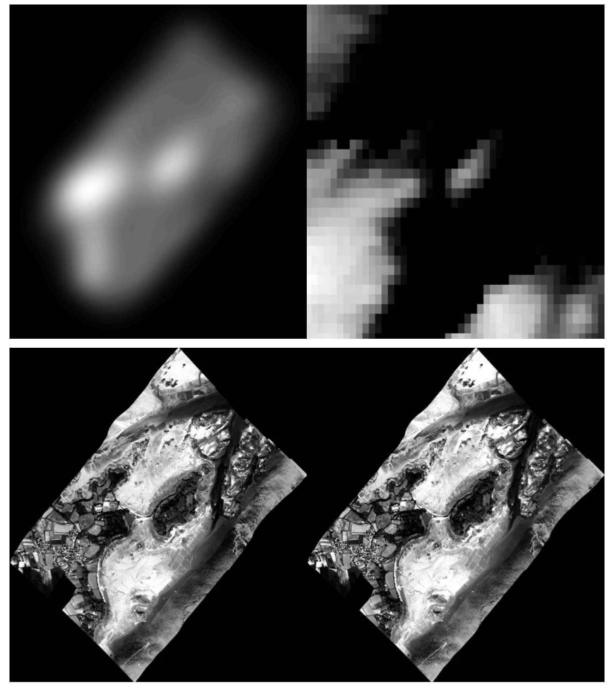

Fig. 3. Automatic mosaicking of adjacent flight tracks. Top left: final DEM estimate ; top right: SRTM DEM ; bottom left: mosaic without DEM ; bottom right: mosaic with DEM estimation.

[5] G. Palubinskas, R. Mueller, and P. Reinartz, "Mosaicking of optical remote sensing images," in *Proc. IEEE Int. Geoscience and Remote Sensing Symposium, IGARSS 2003*, Toulouse, France, 2003, pp. 3955–3957.

[6] K.C. McGwire, "Mosaicking airborne scanner data with the multiquadric rectification technique," *Photogrammetric Engineering and Remote Sensing*, vol. 64, no. 6, pp. 601–606, June 1998.

[7] N. Haala, D. Fritsch, D. Stallmann, and M. Cramer, "On the performance of digital airborne pushbroom cameras for photogrammetric data processing - a case study," in *International Archives of Photogrammetry and Remote Sensing*, Amsterdam, 2000, vol. 33, part B4/1, pp. 320–331.

[8] P. R. Wolf, *Elements of Photogrammetry (2nd ed.)*, McGraw-Hill, New-York, 1974.

[9] P. Viola and W. Wells, "Alignment by maximization of mutual information," *International Journal of Computer Vision*, vol. 24, pp. 137–154, 1997.

[10] G. Hermosillo, C. Chefd'Hotel, and O. Faugeras, "Variational methods for multimodal image matching," *International Journal of Computer Vision*, vol. 50, no. 3, pp. 329–343, 2002.

[11] A.A. Cole-Rhodes *et al.*, "Multiresolution registration of remote sensing imagery by optimization of mutual information using a stochastic gradient," *IEEE Transactions on Image Processing*, vol. 12, no. 12, pp. 1495–1511, December 2003.

[12] Seamless Data Distribution System, "http://seamless.usgs.gov," .